One-dimensional photonic crystals containing memory-enabling liquid-crystal defect layers

Po-Chang Wu and Wei Lee*
Institute of Imaging and Biomedical Photonics, College of Photonics, National Chiao Tung University, Guiren Dist., Tainan 71150, Taiwan

ABSTRACT

Incorporating liquid crystal (LC) as a defect layer in a photonic crystal (PC) leads to the electrically tunable optical spectrum in defect modes within the photonic band gap. While the LC defect layer has bi- or multi-stable states, the profile of defect modes in each stable state can be preserved permanently without applied voltage, indicating a feature of low power consumption for photonic applications. In this paper, we report on our recent development of optical and spectral properties of multilayer PC structures containing various types of memory-enabling LC (ME-LC), including a bistable chiral-tilted homeotropic nematic (BHN), a bistable chiral-splay nematic (BCSN), a bistable dual-frequency cholesteric LC (DFCLC), a tristable polymer-stabilized cholesteric texture (PSCT), and a tristable smectic-A liquid crystal as a defect layer. The defect modes of the PC/ME-LC cell can be switched to not only the voltage-sustained states but the memory states. As a result, PC/ME-LC cells reveal several features such as the wavelength tunability, transmission tunability and optical bistability or tristability of defect modes that are of potential for realizing tunable and memorable optical devices such as low-power-consumption multichannel filters, light shutters or electrically controllable intensity modulators with green concept.

Keywords: photonic crystals, liquid crystals, optical bistability, optical tristability, green devices

1. INTRODUCTION

Photonic crystals (PCs) have attracted considerable attention from the research field in optics since 1987.[1,2] Owing to the spatially distribution of refractive index as well as the dielectric permittivity, the so-called photonic bandgap (PBG) in which photons are forbidden and localized in designated spectral range is created within the transmission spectrum of PCs. When a defect layer is inserted in a PC to wreck its periodicity, partial defect modes allowing the transmission of light at specific wavelengths will be generated within the PBG. According to such a unique combination, liquid crystals (LCs) is one of the potential materials to serve as the defect layer in PCs for designing tunable photonic devices because of their optical anisotropy that can be varied by external stimuli. In 2002, Ozaki *et al.* proposed the first one dimensional (1D) PC/LC configuration by sandwiching a planar-aligned (PA) LC layer between two identical dielectric multilayers.[3] In this case, a feature of wavelength-tunability of defect modes in this PC/PA-LC cell was demonstrated due to the change in refractive index as well as the optical-path-length manipulated by the electric field. Based on this hybrid PC/PA-LC structure, several approaches, such as placing the cell between crossed polarizers,[4,5] varying the incident angle of light[6] and temperature[7] to adjust the optical anisotropy of LCs, have successively been proposed to investigate tunable optical properties of defect modes. Moreover, alluring features of 1D PCs containing various types of LC modes, such as cholesteric LC (CLC),[8,9] in-plane switching (IPS) mode,[10] and twist nematic (TN) mode,[11] have individually been found in accordance with the corresponding operation principle of LC modes and potential applications of these 1D PC/LC structures have also been addressed.

In contrast to aforementioned PC/LC structures, we have designed hybrid structures containing 1D PCs infiltrated with memory-enabling LC (ME-LC) as the defect layer very recently.[12–16] ME-LC is a classification of LC modes that possesses two or multistable memory states; they are switchable from one to another by applied voltages. Thus, the PC/ME-LC cell provides a new notion for designing photonic devices with green concept owing to the fact that the spectral properties of defect modes in a memory state preserve permanently after removal of external field. Based on our

*wlee@nctu.edu.tw; phone +886 (0)6 303-2121; fax +886 (0)6 303-2535

Liquid Crystals XVII, edited by Iam Choon Khoo, Proc. of SPIE Vol. 8828, 88280G
 · doi: 10.1117/12.2023420

recent development of various PC/LC hybrid structures, in this paper, we present spectral and optical properties of multilayer PC structures containing a bistable chiral-tilted homeotropic nematic (BHN) layer, a bistable chiral-splay nematic (BCSN), a bistable dual-frequency cholesteric LC (DF-CLC) layer, a tristable polymer-stabilized cholesteric texture (PSCT), and a tristable smectic-A (SmA) LC as a defect layer. Furthermore, tunability on the wavelength or light-intensity and multistabiltiy of defect modes in each 1D PC/ME-LC cells are demonstrated. Key findings of these 1D PC/ME-LC cells for photonic applications are also clarified.

2. CELL CONFIGURATION

The 1D PC/ME-LC hybrid cell was consisted of two identically indium-tin-oxide (ITO)-coated dielectric multilayers separated by a ME-LC defect layer with a certain thickness d. Depending on the used ME-LC, each dielectric multilayer was coated with proper alignment film, as illustrated in Fig. 1. The dielectric multilayer, regarding as 1D PC structure, was composed of alternative stacking of high refractive index material (Ta_2O_5; refractive index n_H = 2.18) and low refractive index material (SiO_2; n_L = 1.47). The numbers of layer of Ta_2O_5 and SiO_2, depositing on the substrate, were 4 and 5, respectively. The layer thickness of Ta_2O_5 and SiO_2 were 68.09 nm and 102.37 nm. As a result, the PBG of the 1D PC has profiles of central wavelength of ~600nm and width of 290 nm, ranging from 470 to 740 nm.[12] In this study, five different types of ME-LC (i.e., BHN, BCSN, DFCLC, PSCT, and Smectic A LC) were individually employed as the defect layer. The experimental conditions for these five ME-LC defect layers are briefly described as follows[17]: The BHN, BCSN, DFCLC, and PSCT with certain values of helical pitch were made of mixtures of dual-frequency LC (DFLC; MLC-2048, Merck) and left-hand chiral agent (S-811, Merck) under specific concentrations. The values of the cell-thickness-to-pitch ratio were set around unity for BHN and 0.25 for BCSN to correspondingly form two equilibrium stable states. On the other hand, since CLC is a 1D PC structurally, values of central reflection wavelength for DFCLC and PSCT were set to locate in infrared range to avoid affecting the profile of PBG of multilayers. PSCT is a special case of DFCLC having the distribution of polymer networks. In addition to the required monomer and photoinitiator for carrying out the process of photo-polymerization, other experimental conditions of PSCT are the same as those of DFCLC.[15] For the SmA LC layer, the material used was the polymorphic LC 8CB having a phase transition sequence of Cr 21°C SmA 33.5 °C N 40.5 °C. The alignment conditions are tilted-homeotropic with a pretilt angle of approximately 70° and anti-parallel rubbing for BHN, and planar with parallel rubbing for BCSN, and planar with anti-parallel rubbing for DFCLC, PSCT and SmA. Particularly, the DFLC is a class of LC material that has a so-called crossover frequency f_c to distinguish the behavior of dielectric anisotropy $\Delta\varepsilon$. The value of $\Delta\varepsilon$ of DFLC is positive when the voltage with low frequency ($f_1 < f_c$) is applied. In the contrary, applying a high-frequency voltage pulse ($f_2 > f_c$) to the material leads to the negative value of $\Delta\varepsilon$.[18] Owing to this unique characteristic, the switching between stable states in BHN[19] and BCSN[20] is accomplished by frequency-revertible dielectric anisotropy of the DFLC together with the flow effect of LC molecules. On the other hand, for the DFCLC as well as PSCT, using DFLC as the host material in CLC enables the direct two-way switching between stable cholesteric states, yielding an advantageous feature of fast response.[21]

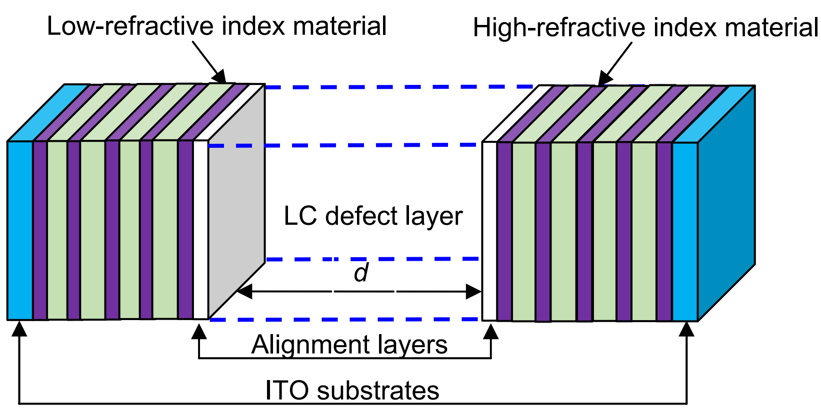

Figure 1. Schematic illustration of the configuration of 1D PC containing ME-LC as a defect layer.

3. OPTICAL PROPERTIES OF DEFECT MODES IN 1D PC/ME-LC CELLS

3.1 Bistable switching and electrical tuning of defect modes in PC/BCSN and PC/BHN cells

BCSN is a kind of dual-mode LC, meaning that it can be operated in either the dynamic mode or the memory mode. According to the operating mechanism of BCSN,[20] the switching between two optically stable states—splay and twist states, represents the memory mode BCSN whereas continuous reorientation of LC molecules from between two voltage-sustained states—the low- and high-tilted bend states, as a function of applied voltage indicates dynamic mode BSCN. Figure 2(a) shows the transmission spectrum of the PC/BCSN cell in four different states without employing any polarizer. Owing to the different contribution of ordinary (n_o) and extraordinary (n_e) refractive indices to the resulting effective refractive index n_{eff} in these states, four specific profiles of defect modes corresponding to the four switchable states in the PC/BCSN cell are obtained. The values of n_{eff} in the splay, twist and low-tilted bend states are attributed to both the n_o and n_e whereas the n_{eff} in the high-tilted bend state (i.e., the homeotropic state) is dictated only by n_o. Consequently, the optical properties of cell in high-tilted bend state reveals less defect mode peaks and plainer spectrum than those in the other states. The result shown in Fig. 2(a) also implies the feature of low power consumption because two sets of defect modes with different optical properties are preserved permanently after removal of applied voltage when the cell is operated in memory mode. Furthermore, considering the operation of PC/BCSN cell in dynamic mode, Fig. 2(b) depicts the voltage-dependent wavelength of four specific defect modes, measured with a single polarizer set between the light source and the cell. The E-mode and O-mode represent the transmission axis of polarizer that is parallel and perpendicular to the rubbing direction of the cell. In the case of E-mode, blue-shift of defect modes in the bend state with increasing voltage results from the decrease of n_e in contribution to the n_{eff}. Such a result indicates the ability of electrical wavelength tunability for the PC/BHN cell. On the other hand, the defect mode peaks in the O-mode do not retain as a constant in principle but shift slightly to shorter wavelength when the applied voltage increases. This phenomenon is attributable to the field-induced substrate distortion in the central region of the cell, which has been confirmed by our recent research.[16]

With similar mechanism of the bistable switching but difference in molecular orientation, the 1D PC/BHN cell possesses two optically stable states—tilted-homeotropic (tH) and tilted-twist (tT) states, and two voltage-sustained states—biased-homeotropic (bH) and biased-twist (bT) states, all switchable under the application of designed voltage pulses.[20] Therefore, four dissimilar profiles of defect modes in the PC/BHN cell are obtained in the transmission spectrum.[12] For the PC/BCSN cell, the dynamic switching from tH to bH states and in bT state are suggested by applying the voltage pulses with frequencies of f_1 and f_2, respectively. In the case of the two homeotropic states (i.e., tH and bH states), as shown in Fig. 3(a), the profile of defect modes in the bH is dictated by the sole n_o; thus, the peaks in the tH states that do not overlap those in the bH state, are clarified as the extraordinary defect modes. Once a high voltage pulse with frequency of f_1 is applied to completely switch the cell from tH to bH state, all extraordinary defect modes vanish. Naturally turning the voltage off enables the reproduction of these defect modes via the relaxation from bH to the stable tH state. Such an operation provides a pathway for this PC/BHN cell in application as a light shutter.

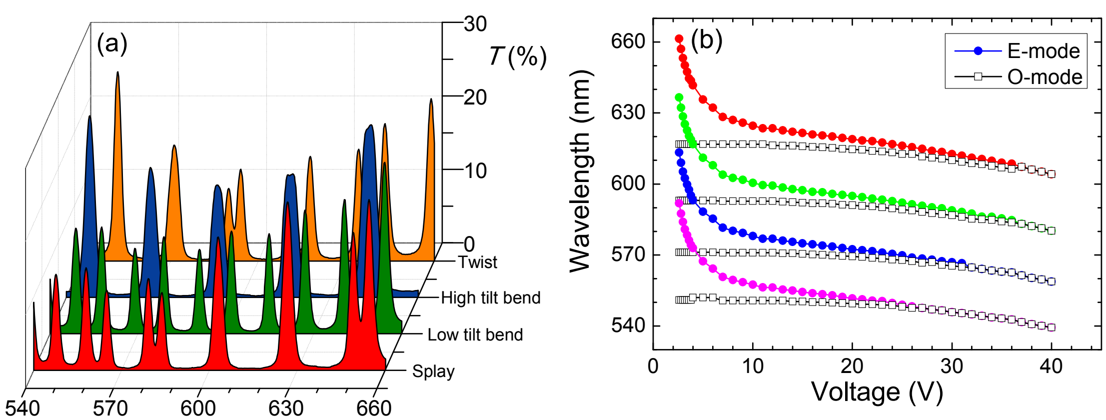

Figure 2. (a) Transmission spectra of the 1D PC/BCSN cell in four different states without any polarizer and (b) Voltage-dependence of four selected defect modes in the bend state with a single polarizer. The E-mode and O-mode represent the transmission axis of the polarizer set parallel and perpendicular to the rubbing direction of the cell, respectively.

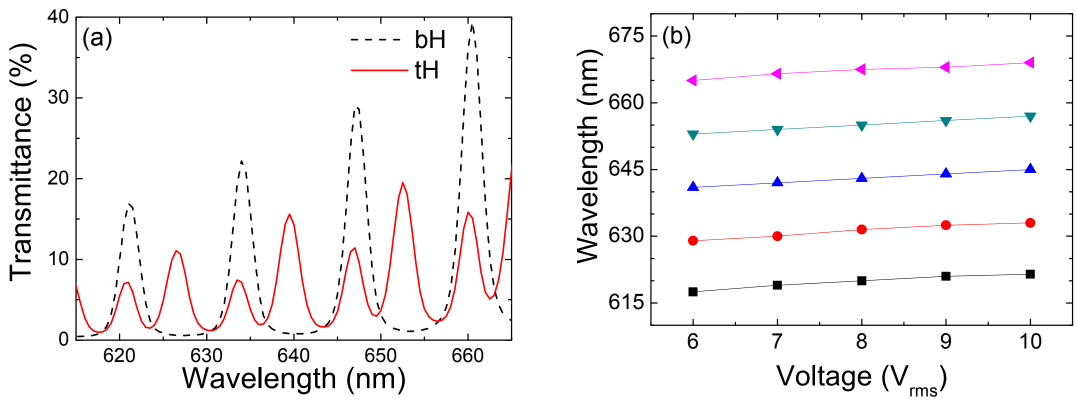

Figure 3. (a) Transmission spectra in the bH and tH states and (b) defect-mode shifts in the bT state with increasing voltage of the 1D PC/BHN cell without any polarizer [12].

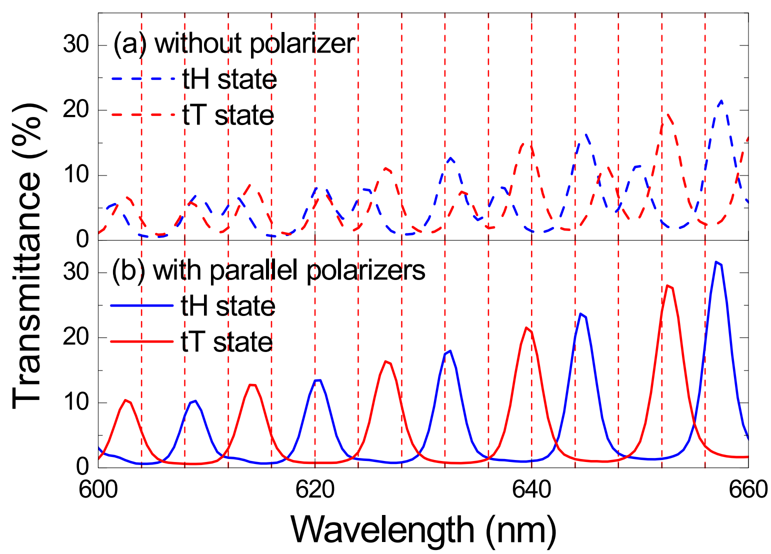

Figure 4. Transmission spectra of a PC/BHN cell under conditions of (a) no polarizers and (b) with parallel polarizers [12].

On the other hand, the wavelength tunability of the defect modes can also be realized in the bT state by applying a voltage pulse with frequency of f_2 to the cell. As shown in Fig. 3(b), redshift of the defect modes is observed due to the increase in n_e, dictated by the decrease in the tilted angle of LC molecules with increasing voltage strength in the bT state.

With further discussion of the bistable switching of defect modes in the two stable states, Fig. 4 displays the transmission spectra of a PC/BHN in tT and tH states with/without the set of parallel polarizers. It have been explained in this paper that the contribution of n_{eff} to the optical profile of defect modes without any polarizers includes both the components of n_o and n_e, except for the cell in the homeotropic state. The defect modes in the tH and tT states are thus intermixed and hardly be resolved, as shown in Fig. 4(a). When the cell is positioned between two parallel polarizers with their transmission axes parallel to the rubbing direction of the cell, the extraordinary defect modes are independently discriminated.[5,11] As a result, two divided sets of defect modes corresponding to the two stable states are obtained in the cell with null voltage under the condition of parallel polarizers (Fig. 4(b)). Moreover, compared with the spectra as shown in Fig. 4(a), the transmittance of each defect-mode peak for the cell with parallel polarizers is obviously promoted, suggesting the cause of superposition of an ordinary and an extraordinary defect modes.[5] This unique result provides a new notion on designing PC/BHN for multichannel photonic applications featuring energy saving.

3.2 Direct two-way switching of defect modes in PC/DFCLC and PC/PSCT cells

Optical bistability is one of many attractive properties of CLCs.[22,23] Typically, the two stable states in CLCs are the transparent planar (P) and light-scattering focal conic (FC) states. (The state characterized by the finger print texture can be obtained when the ratio of the cell gap to the pitch is within a specific range. It can be regarded as a special case of the FC state.) Switching from the P to FC states can directly be accomplished by increasing the amplitude of applied voltage, but an intermediate state—say, the voltage-sustained homeotropic (H) state—is essential for achieving the backward switching from the FC to P state. This means that the switching between the two stable states is not a direct two-way switching.

Recently, we have demonstrated that using DFLC as the host material in a CLC matrix allows direct two-way switching between the P state and the FC state in a cell due to its intrinsic material property of the frequency-revertible dielectric anisotropy.[21,23] According to the operation scheme for the above-mentioned DFCLC as illustrated in Fig. 5, Fig. 6 depicts the transmission spectra of a 1D PC/DFCLC in the P, FC, and H states. Here, both f_1 (= 1 kHz) and f_2 (= 100 kHz) represent the frequencies that are lower and higher than the crossover frequency f_c of the DFLC, respectively. Thus, when a voltage pulse is applied to a DFCLC cell, $\Delta\varepsilon$ is positive at f_1 and negative at f_2. In addition, no polarizer is employed in the measurement of the transmission spectrum. Consider an initial P state in the DFCLC layer. The transmittance spectra of a PC/DFCLC reveal a certain number of defect modes with intensities around 20 to 60% within the PBG (Fig. 6(a)). As a voltage pulse of V_1 = 20 V_{rms} at f_1 is applied to switch the cholesteric texture from the P to FC state, the resulting light scattering attributable to the formation of randomly oriented poly-domains restrains the light transmitted through the cell and the transmittance of the defect-mode peaks is thus as low as ~1% (Fig. 6(b)). When a voltage pulse of V_2 = 35 V_{rms} at f_1 is provided, the formation of H state transferred from either the P and FC states is realized and its corresponding transmission spectrum shows the most intense defect modes (Fig. 6(c)). Note that the reverse switchings; namely, the FC-to-P and H-to-P transitions, can be realized or induced directly by applying voltage pulses of V_3 and V_4 at f_2, respectively (see Fig. 5). In addition, since the value of $\Delta\varepsilon$ is a function of the frequency, direct switching among the P, FC, and H states in a cell can be achieved as well upon application of voltage pulses of varying frequencies at a fixed pulse amplitude.[15] In comparison with spectral profiles of the cell between the P and the H states, the wavelength shifts of the defect-mode peaks are clearly observed due to the change in refractive index between ~ $(n_o + n_e)/2$ and n_o. Moreover, switchings between P and FC states, and between H and FC states enables the switch-on and switch-off of transmissive intensity of defect modes in a cell, suggesting a potential application for PC/DFCLC cell in light shutter. While using PSCT to substitute DFCLC as the defect layer, the optical profiles of the PC/PSCT in the three cholesteric states are quite similar to those of a PC/DFCLC. Noticeably, as far as the potential for realizing green devices is concerned, the tristable PC/PSCT structure is more advantageous since all their three switchable states (P, FC, and H states) are optically stable.

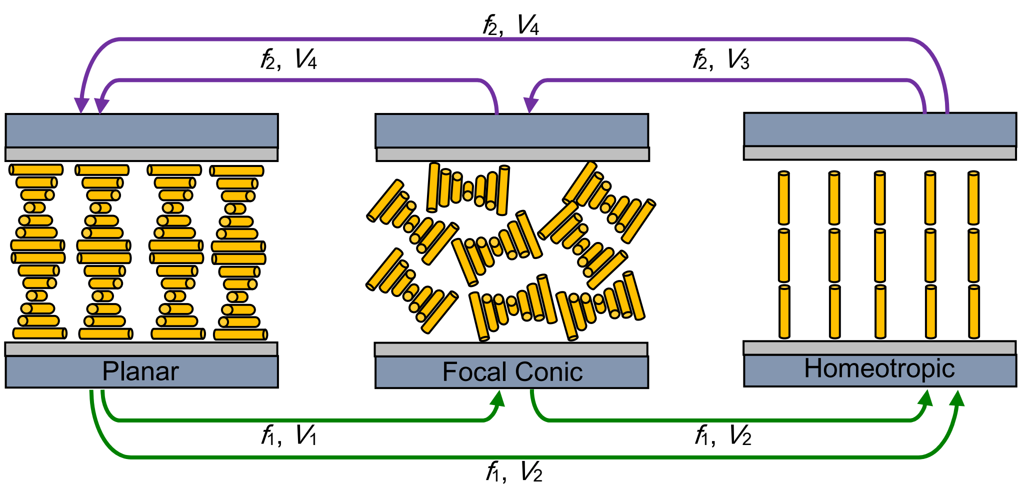

Figure 5. Illustration of the switching mechanism for a DFCLC cell by frequency-modulated voltage pluses.

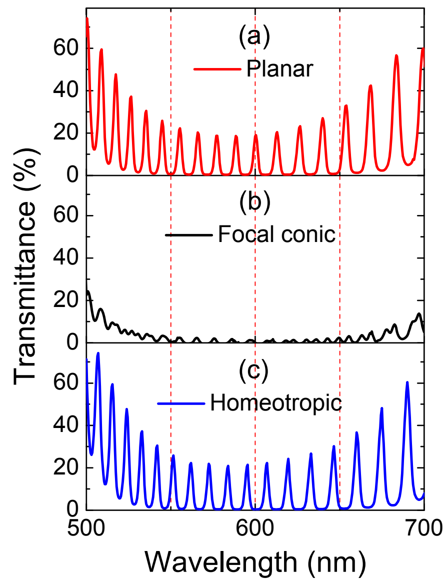

Figure 6. Transmission spectra of the PC/DFCLC in the photonic bandgap in three switchable states. The device is driven by various voltages of (a) 0 V, (b) 20 V_{rms}, and (c) 35 V_{rms} at 1 kHz. (Adopted from [14].)

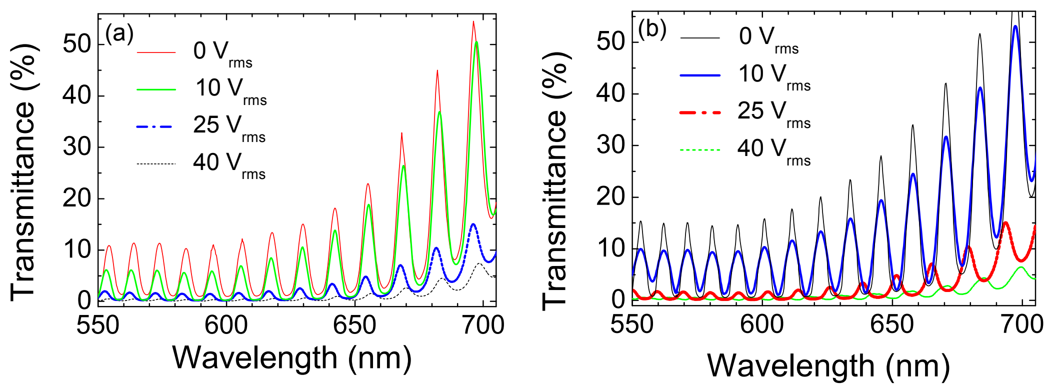

Figure 7. Transmittance of a PC/PSCT cell in the PBG induced by various voltage pulses at fixed frequencies of (a) f_2 = 100 kHz and (b) f_1 = 1 kHz. (After [15].)

Furthermore, light-intensity tunability of defect modes can be performed readily in either the PC/DFCLC or PC/PSCT by modulating the amplitude or frequency of the applied voltage pulse. By using the PC/PSCT cell as an example, Fig. 7 reveals the optical properties of defect modes within the wavelength range from 550 to 700 nm at various voltage pluses. In the PSCT, the initial state at null voltage is the H state. Upon applying f_2 pulse of voltages with increasing amplitude from 0 to V_3 = 40 V_{rms}, the cholesteric state transfers from the H state to the H-FC mixed (HFM) state at 10 and 25 V_{rms} and it then goes into the FC state at 40 V_{rms}. Consequently, the transmitted intensity associated with each defect mode of a PC/PCST cell decreases with increasing amplitude of the voltage pulse due to the H–HFM–FC transition (Fig. 7(a)). If further increasing the applied voltage to V_4 = 60 V, a planar state will be formed and stabilized in the cell after removal of the voltage. Note that the backward switching from P to FC can be carried out here by connecting a voltage pulse with f_1 = 1 kHz at V_1 = 40 V. As shown in Fig. 7(b), the electrical tunability of the strength of the defect-mode peaks results from the existence of P-FC mixed states within the P-to-FC transition by increasing voltage. It is worth mentioning that all the HFM and PFM states are metastable states which can be maintained by several hours in the PC/PSCT cell while the voltage being removal. As a result, alluring features of electrical tunability and optical tristability of the defect-mode peaks in PC/PSCT enable the design of polarizer-free multichannel photonic devices, such as wavelength filter and light shutter, light-intensity modulator with low power consumption.

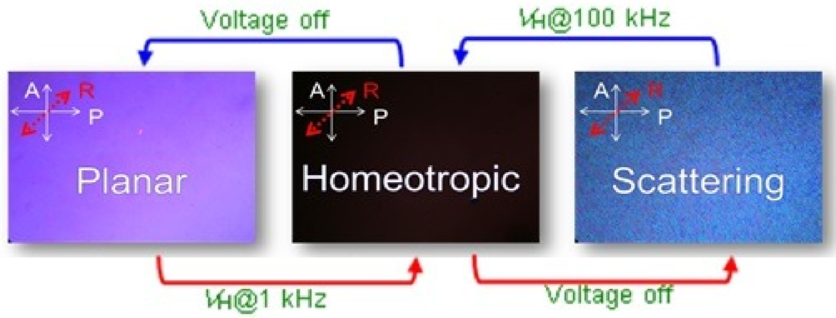

Figure 8. Microscopy images of a SmA LC cell in the P, H, and S states set between crossed polarizers at 29 °C. V_H denotes an adequate voltage for the transformation from either the P or S to the H state. The arrows represent the transmission axes of the polarizer (P) and analyzer (A) as well as the rubbing direction (R). (Adapted from [16].)

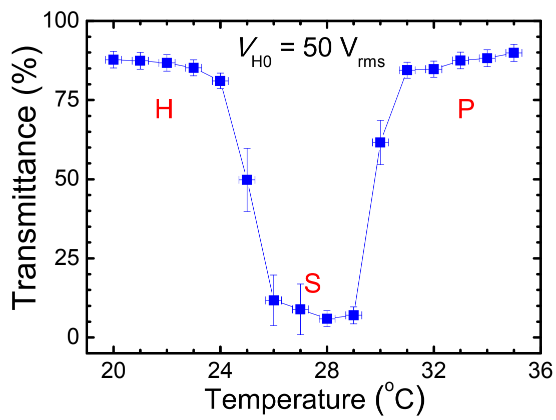

Figure 9. Temperature dependence of transmission of tristable SmA LCs with an applied short-pulse voltage at wavelength of 540 nm [16].

3.3 Thermally/Electrically induced tristability in a PC/SmA cell

Memory-enabling SmA LC cell was first demonstrated in 1978.[24] By preparing such a cell with homeotropic alignment, it is bistable in the scattering (S) and homeotropic (H) states, induced electrically by applying low- and high-frequency voltages. Other groups have concerned the composite of a SmA LC doped with an ionic additive and demonstrated not only the bistable S-to-H switching but multistable operations between S and H states.[25] The mechanisms of bistable switching of aforementioned examples are quite the same since the low-frequency voltage applied to the cell is used to induce dielectric instability of LC molecules, resulting in the formation of the stable S state. In our proposed tristable SmA cell, the stable states, including the S, H, and the planar (P) state, can be obtained by using not only frequency-modulated voltage pluses but by varying surrounding temperature T. Figure 8 depicts the scheme for switching between P and S, and the resulting microscopic images of the three stable states under a polarizing optical microscope at temperature $T = 29$ °C. Owing to the planar-antiparallel cell configuration, the initial state of the SmA cell is essentially the P state. Application of a voltage with a sufficient amplitude (V_H) at 1 kHz to the cell induces the reorientation of the smectic layer as well as the LC molecules with the layer normal and molecular axis perpendicular to the substrate and thus forms a voltage-sustained H state. After turning off the voltage, the competition between the anchoring energy and homeotropic inertia of LCs molecules, attributed to the forces by initial planar geometry and smectic layering, leads to the random LC molecular alignment, thereby yielding the stable S state. Specifically, applying a high-frequency voltage pulse can supply considerable joule heat and, in turn, backwardly switch the cell from the S to the optically stable P state through a cycling of LC phase transition followed by natural cooling of the material. Figure 9 displays the temperature dependence of transmittance of a tristable SmA at the wavelength of 540 nm after removal of an agitating voltage pulse $V_{H0} = 50$ V. Note that the symbol V_{H0} means the state of voltage being turned off from a 1 kHz pulse initially applied to create the H state. The variation of transmission indicates the state-change of the SmA LC bulk. In the temperature range between 31 and 33 °C, the SmA LC bulk exhibits the optically stable P state through relaxation from the H state due to the weakened smectic layering in the temperature range near the SmA–N phase transition temperature. Noticeably, the SmA cell exhibits a stable H state after removal of a 50V pulse at 1 kHz below 25 °C by the increase in the strength of the smectic layering with descending temperature. This result suggest that the temperature plays a crucial role in obtaining a specific tristable state after the agitation of V_{H0}. By using the dependency of temperature on the stability of smectic layering, it is suggested that the stable H state can be switched to either S or P state by increasing the surrounding temperature to an appreciated value. Figure 10 shows the temperature-dependent state transformation.

Based on the switching mechanism for a tristable SmA-LC mentioned above, Fig. 11 demonstrates the wavelength and transmission tunability of defect modes in the transmission spectra of a 1D PC/SmA cell by various applied voltage

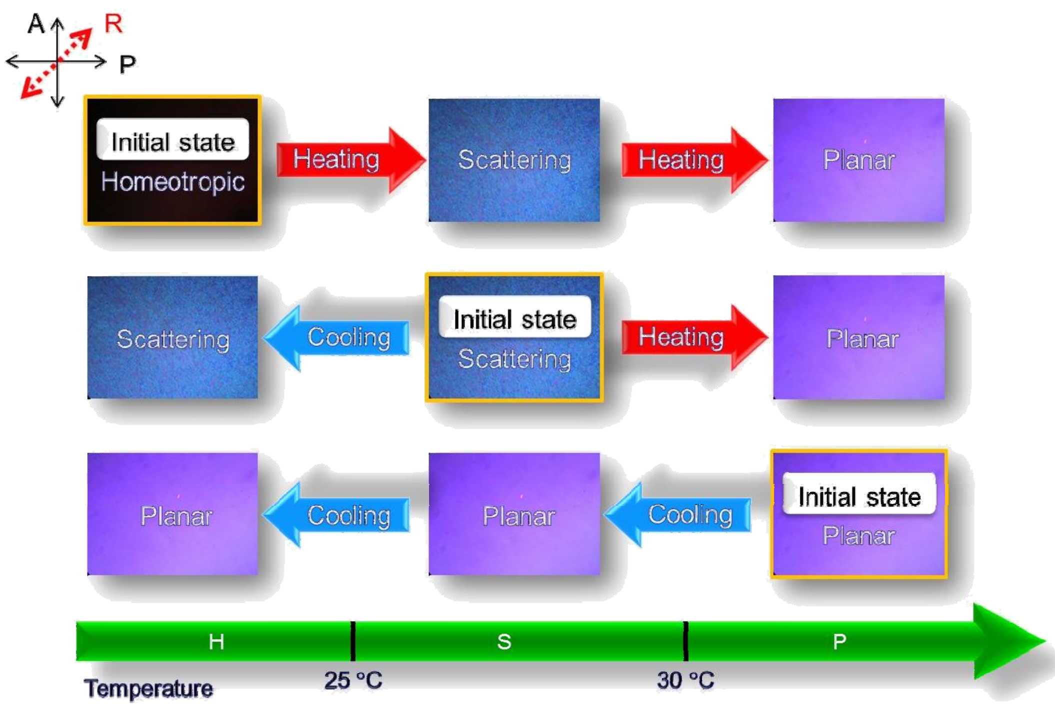

Figure 10. State transformation of a SmA cell from various initial conditions due to the ambient temperature change.

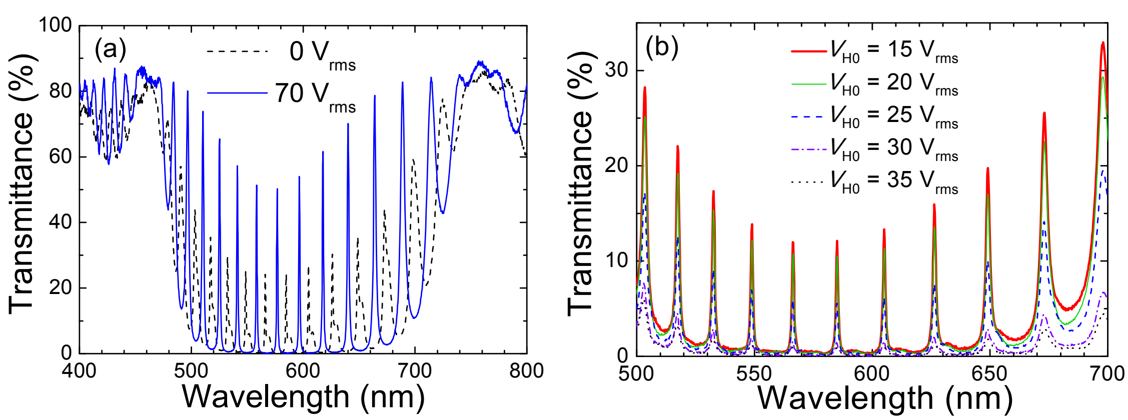

Figure 11. Transmittance spectra of a 1D PC/SmA cell in (a) the stable P (0 V_{rms}) and voltage-sustained H (70 V_{rms}) states and in (b) mixed states induced by various voltage pluses at 1 kHz. (After [16].)

pulses. As shown in Fig. 11(a), it can clearly be distinguished that the defect modes in the stable P state (at 0 V_{rms}) blue-shift to those in the voltage-sustained H state (at 70 V_{rms}) due to the decrease in the overall optical path length as well as the effective refractive index. On the other hand, the P-to-S switching can be achieved by a voltage of V_{H0} at 1 kHz. Because the strength for light-scattering in the S state depends on the value of V_{H0},[16] the strength of light intensity of the defect mode signals in a PC/SmA-LC cell can undoubtedly be modulated (Fig. 11(b)). On the basis of the identical tunability and the optical tristability of defect modes, this tristable PC/SmA-LC cell is as powerful as the PC/PSCT for uses in designing various photonic devices with green concept.

4. CONCLUSION

In conclusion, optical properties of five types of 1D PC/ME-LC cell have been reported. Potential uses of each cell have been suggested in accordance with its fascinating attributes for designing photonic devices. For PC/BCSN and PC/BHN cells, three and four sets of defect modes with distinct optical profiles were individually found in their stable and voltage-sustained states, switched by frequency-modulated voltage pluses associated with the flow effect of LC molecules. In addition, electrical wavelength-tunability of defect modes can be realized while dynamic switching the cells. With increasing voltage amplitude, the dynamic switching of defect modes reveals blue-shift in the bend state of PC/BCSN and red-shift in the biased-twist state of PC/BHN owing to the change of refractive index. Particularly, clear separation of two sets of defect modes with independent optical profile is achieved in the two stable states (tT and tH states) of the PC/BHN cell by further employing a set of parallel polarizers; thus, implying an new notion for designing a multichannel wavelength filter as a green device.

On the other hand, based on our previous development of DFCLC, a bistable PC/DFCLC and a tristable PC/PSCT were successively developed. In these two types of cells, switchings among the P, FC and H states are direct and reversible by either the frequency- or amplitude-modulated voltage pulse determined by the material properties of the DFLC. In view of the transmission spectrum of these cells in each state, the transmissive intensity of the defect modes in the scattering FC state is quite low (< 1%) whereas it is relatively intense in either the transparent P or H state. Moreover, the refractive-index difference between the P and H states demonstrates the shift of defect modes in the transmission spectra.

For the development of memory-enabling SmA LC, a new design of the tristable SmA mode was proposed. The mechanism have been clarified for achieving the stable P, S, and H states in a SmA cell by frequency-modulated voltage pulse and/or temperature. By incorporating this tristable SmA as a defect layer in a 1D PC, the resulting optical spectrum reveals not only the optical tristability but bi-functional tunability for the defect modes. As a result, PC/DFCLC, PC/PSCT as well as PC/SmA exhibit luring features of electrical wavelength-tunability, intensity-tunability, and bi- or tri-stability of defect modes, making them suitable for creating polarizer-free multichannel photonic devices, such as light shutters, wavelength filters, and intensity modulators, with low power consumption.

ACKNOWLEDGEMENTS

The authors are grateful for the financial support from the National Science Council of the Republic of China (Taiwan) under grant Nos. NSC 101-2112-M-009-018-MY3 and NSC 101-2811-M-009-059.

REFERENCES

[1] Yablonovitch, E., "Inhibited spontaneous emission in solid-state physics and electronics," Phys. Rev. Lett. 58(20), 2059–2062 (1987).
[2] John, S., "Strong localization of photons in certain disordered dielectric superlattices," Phys. Rev. Lett. 58(23), 2486–2489 (1987).
[3] Ozaki, R., Matsui, T., Ozaki, M. and Yoshino, K., "Electro-tunable defect mode in one-dimensional periodic structure containing nematic liquid crystal as a defect layer," Jpn. J. Appl. Phys. 41, L1482–L1484 (2002).
[4] Zyryanov, V. Ya., Gunyakov, V. A., Myslivets, S. A., Arkhipkin, V. G. and Shabanov, V. F., "Electrooptical switching in a one-dimensional photonic crystal," Mol. Cryst. Liq. Cryst. 488, 118–126 (2008).

[5] Zyryanov, V. Ya., Myslivets, S. A., Gunyakov, V. A., Parshin, A. M., Arkhipkin, V. G., Shabanov, V. F. and Lee, W., "Magnetic-field tunable defect modes in a photonic-crystal/liquid-crystal cell," Opt. Express 18(2), 1283–1288 (2010).
[6] Arkhipkin, V. G., Gunyakov, V. A., Myslivets, S. A., Zyryanov, V. Ya. and Shabanov, V. F., "Angular tuning of defect modes spectrum in the one-dimensional photonic crystal with liquid-crystal layer," Eur. Phys. J. E 24, 297–302 (2007).
[7] Arkhipkin, V. G., Gunyakov, V. A., Myslivets, S. A., Gerasimov, V. P., Zyryanov, V. Ya., Vetrov, S. Ya. and Shabanov, V. F., "One-dimensional photonic crystals with a planar oriented nematic layer: Temperature and angular dependence of the spectra of defect modes," JETP 106, 388–398 (2008).
[8] Matsuhisa, Y., Ozaki, R., Yoshino, K. and Ozaki, M., "High Q defect mode and laser action in one-dimensional hybrid photonic crystal containing cholesteric liquid crystal," Appl. Phys. Lett. 89(10), 101109 (2006).
[9] Ozaki, R., Matsui, T., Ozaki, M. and Yoshino, K., "Electrically color-tunable defect mode lasing in one-dimensional photonic-band-gap system containing liquid crystal," Appl. Phys. Lett. 82(21), 3593–3595 (2003)
[10] Ozaki, R., Ozaki, M. and Yoshino, K., "Defect mode in one-dimensional photonic crystal with in-plane switchable nematic liquid crystal defect layer," Jpn. J. Appl. Phys. 43(11B), L1477–L1479 (2004).
[11] Lin, Y.-T., Chang, W.-Y., Wu, C.-Y., Zyryanov, V. Ya. and Lee, W., "Optical properties of one-dimensional photonic crystal with a twisted-nematic defect layer," Opt. Express 18(26), 26959–26964 (2010).
[12] Wu, C.-Y., Zou, Y.-H., Timofeev, I., Lin, Y.-T., Zyryanov, V. Ya., Hsu, J.-S. and Lee, W., "Tunable bi-functional photonic device based on one-dimensional photonic crystal infiltrated with a bistable liquid-crystal layer," Opt. Express 19(8), 7349–7355 (2011).
[13] Hsiao, Y.-C., Zou, Y.-H., Timofeev, I. V., Zyryanov, V. Ya and Lee, W., "Spectral modulation of a bistable liquid-crystal photonic structure by the polarization effect," Opt. Mater. Express 3(6), 821–828 (2013).
[14] Hsiao, Y.-C., Wu, C.-Y., Chen, C.-H., Zyryanov, V. Ya. and Lee, W., "Electro-optical device based on photonic structure with a dual-frequency cholesteric liquid crystal," Opt. Lett. 36(14), 2632–2634 (2011).
[15] Hsiao, Y.-C., Hou, C.-T., Zyryanov, V. Ya. and Lee, W., "Multichannel photonic devices based on tristable polymer-stabilized cholesteric textures," Opt. Express 19(24), 7349–7355 (2011).
[16] Chen, C.-H., Zyryanov, V.-Y. and Lee, W., "Switching of defect modes in a photonic structure with a tristable smectic-A liquid crystal," Appl. Phys. Express 5, 082003 (2012).
[17] Wu, P.-C. and Lee, W., "Tunable and memorable optical devices with one-dimensional photonic-crystal/liquid-crystal hybrid structures," in [Optical Devices in Communication and Computation], edited by Peng Xi, InTech, Croatia, Chap. 4, pp. 55–80 (2012), ISBN 978-953-51-0763-7. Open access at http://www.intechopen.com/books/optical-devices-in-communication-and-computation.
[18] Xianyua, H., Wu, S.-T. and Lin, C.-L., "Dual frequency liquid crystals: a review," Liq. Cry. 36, 717–726 (2009).
[19] Hsu, J.-S., Liang, B.-J. and Chen, S.-H., "Bistable chiral tilted-homeotropic nematic liquid crystal cells," Appl. Phys. Lett. 85, 5511–5513 (2004).
[20] Yao, I.-A., Yang, C.-L., Chen, C.-J., Pang, J.-P., Liao, S.-F., Li, J.-H. and Wu, J.-J., "Bistability of splay and π-twist states in a chiral-doped dual frequency liquid crystal cell," Appl. Phys. Lett. 94, 071104 (2009).
[21] Hsiao, Y.-C., Tang, C.-Y. and Lee, W., "Fast-switching bistable cholesteric intensity modulator," Opt. Express 19(10), 9744–9749 (2011).
[22] Xu, M. and Yang, D.-K., "Dual frequency cholesteric light shutters," Appl. Phys. Lett. 70(6), 720–722 (1997).
[23] Berreman, D. W. and Heffner, W. R., "New bistable cholesteric liquid-crystal display," Appl. Phys. Lett. 37, 109–111 (2006).
[24] Coates, D., Crossland, W. A., Morrisy, J. H. and Needham, B., "Electrically induced scattering textures in smectic A phases and their electrical reversal," J. Phys. D: Appl. Phys. 11, 2025–2034 (1978).
[25] Gardiner, D. J., Morris, S. M. and Coles, H. J., "High-efficiency multistable switchable glazing using smectic A liquid crystals," Sol. Energy Mater. Sol. Cells 93(3), 301–306 (2009).